

Received: 2017.06.01
Accepted: 2017.07.03
Published: 2018.02.08

Hydroxysafflor-Yellow A Induces Human Gastric Carcinoma BGC-823 Cell Apoptosis by Activating Peroxisome Proliferator-Activated Receptor Gamma (PPAR γ)

Authors' Contribution:
Study Design A
Data Collection B
Statistical Analysis C
Data Interpretation D
Manuscript Preparation E
Literature Search F
Funds Collection G

CDEFG 1 **Li Liu***
ABC 1 **Na Si***
DEF 1 **YiCong Ma**
BCD 1 **DongYu Ge**
BCD 1 **Xue Yu**
BCD 1 **AngRan Fan**
BCD 1 **Xu Wang**
DE 1 **JingHong Hu**
DEF 1 **Peng Wei**
FG 1 **ZiWei Chen**
ACDEF 1 **Qian Zhang**
ACDF 2 **CuiLing Feng**

1 School of Traditional Chinese Medicine, Beijing University of Chinese Medicine, Beijing, P.R. China
2 Department of Traditional Chinese Medicine, Peking University People's Hospital, Beijing, P.R. China

* Li Liu and Na Si contributed equally to this work

Corresponding Authors:

Qian Zhang, e-mail: zq19881988@163.com, CuiLing Feng, e-mail: fengcuiling@sina.com

Source of support:

This work was supported by grants from the National Natural Science Foundation of China (30572436 and 81473655)

Background: Anti-tumor properties of hydroxysafflor-yellow A (HSYA) have been recently revealed, as a series of apoptotic factors were confirmed to be regulated by HSYA and associated with peroxisome proliferator-activated receptor Gamma (PPAR γ). In this study, we investigated the cell apoptosis mechanism of HSYA via activated PPAR γ signal in human gastric carcinoma cells.

Material/Methods: BGC-823 cells were cultured and divided into 5 independent groups: Tumor, HSYA, HSYA+PPAR γ inhibitor (GW9662), and PPAR γ agonist (RGZ), RGZ+GW9662. Cell proliferative activity was measured by MTT. Apoptosis and cell cycle were detected by flow cytometry. The nuclear translocation of PPAR γ was detected by immunofluorescence staining chemistry, and mRNA levels of PPAR γ and caspase-3 were measured by real-time qPCR.

Results: Compared to the RGZ group, the HSYA group (100 μ M) showed a similar inhibitory effect on the proliferation process of BGC-823 cells, inducing their apoptosis. As a result, the transition of BGC-823 cells from G0/G1 phase to S phase was blocked. HSYA was also found to promote the nuclear translocation of PPAR γ , leading to increased expression of PPAR γ and caspase-3. The regulatory effect of HSYA on BGC-823 cells could be further inhibited by PPAR γ inhibitor in group GW9662.

Conclusions: We report the inhibitory effect of HSYA on the proliferation of BGC-823 cells, which results in activating PPAR γ -dependent cell cycle blocking and cell apoptosis, suggesting that PPAR γ is a specific type of HSYA that can induce apoptosis of BGC-823 cells.

MeSH Keywords: **Apoptosis • Cancer • Human Gastric Carcinoma BGC-823 Cells • HSYA • PPAR-gamma**

Full-text PDF: <https://www.medscimonit.com/abstract/index/idArt/905587>

 2768

 1

 9

 39



Background

Gastric cancer is one of the most common malignancies of the digestive system, with remarkable features such as poor prognosis and difficult therapy, resulting in high incidence and mortality, especially in China [1]. The traditional therapeutic methods against tumors may cause damage to normal cells, tissues, and organs, and chemotherapy drugs usually lead to adverse reactions, side effects, and drug resistance. Therefore, traditional Chinese medicine is playing an increasingly important role in cancer research and treatment due to its unique advantages.

Blood-activating and stasis-removing Chinese medicine has been shown to not only promote blood circulation but also to remove blood stasis, which provides a potential feasible therapy to eliminate local tumors, improve internal microcirculation, and reduce tumor growth and migration. Among the blood-activating and stasis-removing Chinese medicines, safflower [*Carthamus tinctorius L. (Asteraceae)*] is a representative traditional herb, exhibiting significant anti-tumor activities in esophageal cancer, liver cancer, and stomach cancer [2,3]. Hydroxysafflor-yellow A (HSYA), which has a chalcone glycoside structure, is the main water-soluble active component of safflower. HSYA is reported to have various therapeutic features such as anti-inflammation, anti-tumor, anti-cerebral ischemia injury, and anti-myocardial injury [4–7]. In our previous work, we first reported the inhibitory effects of HSYA on angiogenesis in chick chorioallantoic membrane CAM [8]. The results showed that the number of newly-formed CAM blood vessels was significantly decreased and the vessel walls was induced to thin by HSYA treatment. We have also established an *in vitro* co-culture model of HepG2 human tumor cell line and human umbilical vein endothelial cells (HUVECs). At certain concentrations of HSYA, the abnormal proliferation of endothelial cells apoptosis was significantly stimulated [9], and that of tumor cell culture supernatant-induced (TCCS) endothelial cells was inhibited without affecting normal endothelial cell growth [10,11].

HSYA was also reported to suppress tumor growth by inhibiting cell proliferation [12,13] and angiogenesis [8,14], and inducing cell apoptosis [9,15]. Since many signal factors (e.g., Bcl-2, Bax, and caspase-3) in numerous apoptotic pathways can be mediated by HSYA [9,12,13], it may function as a common molecular target to activate various downstream apoptotic signals and promote tumor cell apoptosis. Moreover, peroxisome proliferator-activated receptor (γ) (PPAR γ) is also associated with these signal factors [16–18].

In light of the above, we hypothesized that HSYA promotes tumor cell apoptosis dependent on the activation of PPAR γ (Figure 1). To verify this hypothesis, we explored the effects

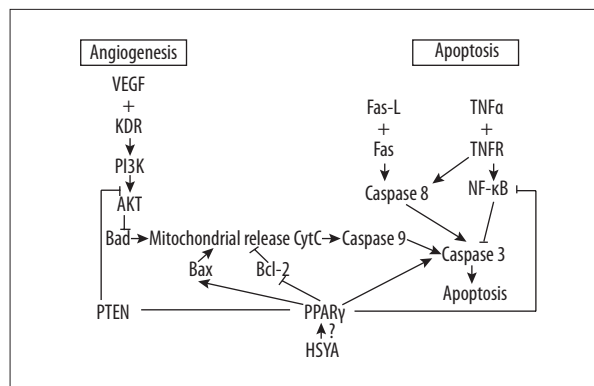


Figure 1. HSYA inhibits angiogenesis and induces tumor cells apoptosis by activating PPAR γ .

of HSYA on BGC-823 cells, including proliferation, cell cycle, and relevant apoptosis factors. The cells were treated with rosiglitazone (RGZ) and GW9662, PPAR γ agonist, and inhibitor, correspondingly.

Material and Methods

Main reagents and materials

HSYA ($C_{27}H_{32}O_{16}$, purity >92.5%) was obtained from China Pharmaceutical and Biological Products, Beijing, CN), and GW9662 and RGZ (purity >99%) were purchased from Abcam. Human gastric carcinoma BGC-823 cells were purchased from the Cancer Hospital of the Chinese Academy of Medical Sciences. Dulbecco's minimal essential medium (DMEM), fetal bovine serum (FBS), and streptomycin-penicillin were from Hyclone. MTT, dimethyl sulfoxide (DMSO), and annexin V-FITC Kit were from Solarbio. PPAR γ and caspase-3 antibodies were purchased from CST. Secondary antibodies were purchased from ComWin Biotech. DAPI was obtained from Biotopped and Trizol was obtained from Invitrogen. The PCR kit was purchased from Roche.

Cell culture and grouping

BGC-823 cells were maintained in DMEM supplemented with 10% FBS and 100 IU/ml of streptomycin-penicillin at 37°C in a humidified atmosphere containing 5% CO $_2$.

When the cells were in the logarithmic growth phase, they were randomly divided into 5 groups: tumor, HSYA, RGZ, HSYA+GW9662, and RGZ+GW9662 groups. Cells were treated with HSYA, GW9662, and RGZ according to the groups above, while tumor group cells were untreated.

Table 1. Primer sequences for real-time quantitative PCR.

Gene name	Forward primer (5'-3')	Reverse primer (5'-3')	Annealing temperature (°C)	Length of product (bp)
PPAR γ	AGGAGCAGAGCAAAGAGG	TAAATGATCTCGTGGACTCCATATT	55	131
Caspase-3	GGCATTGAGACAGACAGT	AACCACCAACCAACCATT		345
GAPDH	TTGGTATCGTGAAGGACT	GGATGATGTTCTGGAGAGC		120

MTT assay

BGC-823 cells were routinely digested and inoculated in 96-well plates at 8×10^3 cells/well. After incubation for 24 h, the cells were treated by different concentrations of HSYA (25, 50, 100, 200, and 400 μ M) for 48 h, then the cells were treated with 20 μ l MTT (5 μ g/ml) for 4 h and dissolved in 120 μ l/well DMSO for 10 min. The absorbance value was measured at 570 nm on a microplate reader (Tecan). The relative cell viability was calculated by the formula: (OD of samples/OD of blank control) \times 100%. The optimal concentration of HSYA was then selected to proceed to the next steps.

The effects of HSYA, RGZ, and GW9662 on the proliferation of BGC-823 cell line were colorimetrically tested by MTT. BGC-823 cells (8×10^3 cells/well) were seeded into 96-well plate and cultured in DMEM for 24 h. Then, the cells were treated by optimal HSYA (100 μ M), RGZ (5 μ M), and GW9662 (10 μ M) separately [18–20]. MTT was added to each well and then dissolved in DMSO. The absorbance value was measured at 570 nm by a microplate reader.

Apoptotic assay

An annexin V-FITC kit was used to quantify the percentage of cells undergoing apoptosis. BGC-823 cells (3×10^5 cells/well) were seeded into 6-well plates and cultured in DMEM for 24 h. Then, the cells were treated with different drugs in each well, as above. These cells were collected and centrifuged at 1000 g for 5 min and then resuspended in 100 μ l of annexin V-FITC mixed with 10 μ l of annexin V-FITC and 10 μ l of PI for 5 min in the dark at room temperature. Finally, these samples were subjected to FACSCalibur flow cytometry (Becton-Dickinson) to quantify the cell apoptosis rate.

Cell cycle analysis

BGC-823 cells (3×10^5 cells/well) were seeded into 6-well plates and cultured in DMEM for 24 h. After being treated with different drugs as above, the cells were centrifuged at 1000 g for 5 min, washed twice with PBS, fixed in 70% ice-cold ethanol, and suspended at 4°C overnight. Then, cells were washed with PBS, centrifuged, and resuspended in 500 μ l RNaseA (50 μ g/ml).

After incubation for 30 min at 37°C, 5 μ l of PI was added and the cells were incubated for 5 min in the darkness. Finally, the cells were tested by FACSCalibur flow cytometry.

Nuclear translocation

BGC-823 cells (2.5×10^4 cells/well) were seeded into 24-well plates containing a glass cover slip in each well and treated with different drugs as above. Slides were air-dried and fixed for 15 min in 4% paraformaldehyde at 37°C. Cells were washed twice with ice-cold PBS, incubated for 10 min in PBS containing 0.25% Triton X-100 at room temperature, washed twice with PBS, immersed in 1% BSA for 30 min, and incubated with PPAR γ antibody diluted 1:300 with 1% BSA overnight at 4°C. Slides were washed with PBS and incubated with secondary antibodies diluted 1:50 with 1% BSA in the dark for 1 h at room temperature. Finally, slides were washed and then immersed in 1 μ g/ml DAPI for 3 min, rinsed, mounted with cover slips using 90% glycerol, and examined qualitatively under a laser scanning confocal microscope (Olympus).

RT-qPCR assay

BGC-823 cells in 6-well plates (4×10^5 cells/well) were treated with different drugs as above. The cells were lysed by Trizol reagent for total RNA. Reverse transcription reaction was performed in a 20- μ l volume containing 2 μ g total RNA. The reaction was carried out using SYBR Green, and I dye technology according to the instructions for the fluorescence quantitation. The real-time polymerase chain reaction (PCR) reaction system (20 μ l) consisted of cDNA (2 μ l), ddH $_2$ O (7 μ l), PCR Mix (10 μ l), and primers (1 μ l) (Table 1). Reduced glyceraldehyde-3-phosphate dehydrogenase (GAPDH) gene was used as an internal control. Cycling parameters were: 95°C for 3 min, 95°C for 10 s, 55°C for 30 s, and 72°C for 30 s, with a total of 40 cycles. PCR reactions and data acquisition were performed using the CFX-96 system (Bio-Rad). The cycle threshold (CT) was recorded and relative mRNA expression of the target gene was calculated using the $2^{-\Delta\Delta CT}$ method.

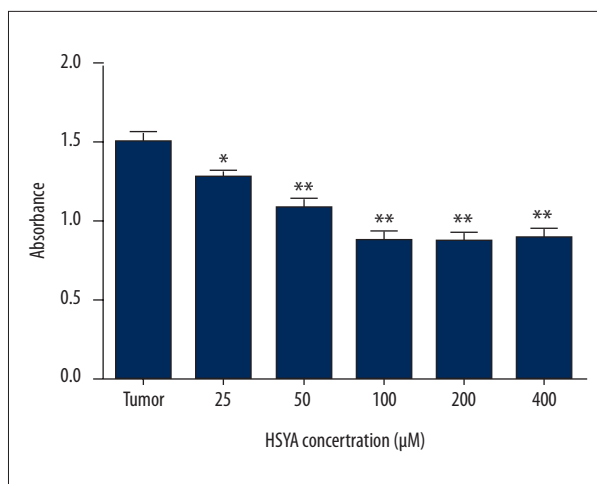


Figure 2. HSYA inhibited the proliferation of human gastric carcinoma BGC-823 cells. Tumor group: human gastric carcinoma BGC-823 cell DMEM medium. Cells in all the other groups were treated with different concentrations of HSYA. MTT assay was performed after treatment for 48 h. Compared with the tumor group, * $P < 0.05$, ** $P < 0.01$ ($n = 5$).

Statistical analysis

All data are expressed as mean \pm standard deviation (SD). Data analysis was performed using the SPSS 20.0 software program (SPSS Inc., Chicago). One-way analysis of variance (ANOVA) and least significant difference (LSD) tests were used for all intergroup comparisons. For all analysis, differences were considered statistically significant when $P < 0.05$; the exact P-values are shown unless $P < 0.01$.

Results

Proliferation of BGC-823 cells is inhibited by HSYA

To test the inhibitory effect and to screen the optimal inhibitory concentration of HSYA on human gastric cancer BGC-823 cells, the cells were treated with HSYA with different concentrations (from 25 μM to 400 μM) for 48 h. MTT assay showed that proliferation of BGC-823 cells was inhibited in a dose-dependent manner by HSYA with concentrations under 100 μM , and the proliferation plateau reached after the concentration of HSYA was above 100 μM (Figure 2). Therefore, 100 μM was chosen as the optimal inhibitory concentration for the following research.

MTT assay was performed to investigate whether HSYA inhibited BGC-823 cell growth by activating PPAR γ . As shown in Figure 3, the proliferation abilities for both HSYA and RGZ groups were dramatically decreased in comparison with the

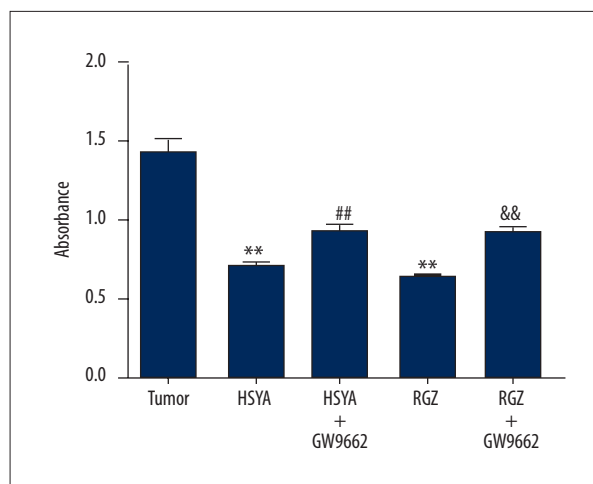


Figure 3. Effect of HSYA on BGC-823 cells proliferative activity of BGC-823 cells treated with drugs at different concentrations: HSYA 100 μM , RGZ 5 μM GW9662 10 μM . Compared with tumor group: ** $P < 0.01$; compared with HSYA group: ## $P < 0.01$; compared with RGZ group: && $P < 0.01$ ($n = 6$).

tumor group ($P < 0.01$), while those for the HSYA+GW9662 group and RGZ+GW9662 group were increased in comparison with the HSYA group and RGZ group, respectively ($P < 0.01$). These results suggest that the inhibitory effect of HSYA on BGC-823 cells was dependent on activated PPAR γ .

Apoptosis of BGC-823 cells is induced by HSYA

Annexin V-FITC/PI assay was then performed to test the apoptosis inductivity of HSYA on BGC-823 cells with activated PPAR γ , and the annexin V-FITC/PI quadrant distribution of the cells in all 5 groups was measured (Figure 4A). We found that

the apoptosis rate of the tumor group was $(6.55 \pm 1.42)\%$, while those of the HSYA group and RGZ group increased to $18.47 \pm 5.46\%$ and $28.97 \pm 7.82\%$, respectively (Figure 4B). A significant difference ($P < 0.01$) was found between these groups and the tumor group. After treatment with GW9662, the apoptosis rates were decreased to $9.90 \pm 1.47\%$ ($P < 0.05$) and $14.44 \pm 1.96\%$ ($P < 0.01$) for the HSYA+GW9662 group and RGZ+GW9662 groups, respectively. These results show that the induced effect of HSYA on apoptosis on BGC-823 cells was dependent on activated PPAR γ .

Cell cycle of BGC-823 cells is blocked by HSYA

To further investigate whether HSYA blocks the cycle of BGC-823 cells by activating PPAR γ , flow cytometry assay was performed. The cell cycle distributions of all 5 groups were mapped (Figure 5). For the tumor group, the majority of cells were in S phase ($61.45 \pm 5.72\%$), while proportions of cells in S phase

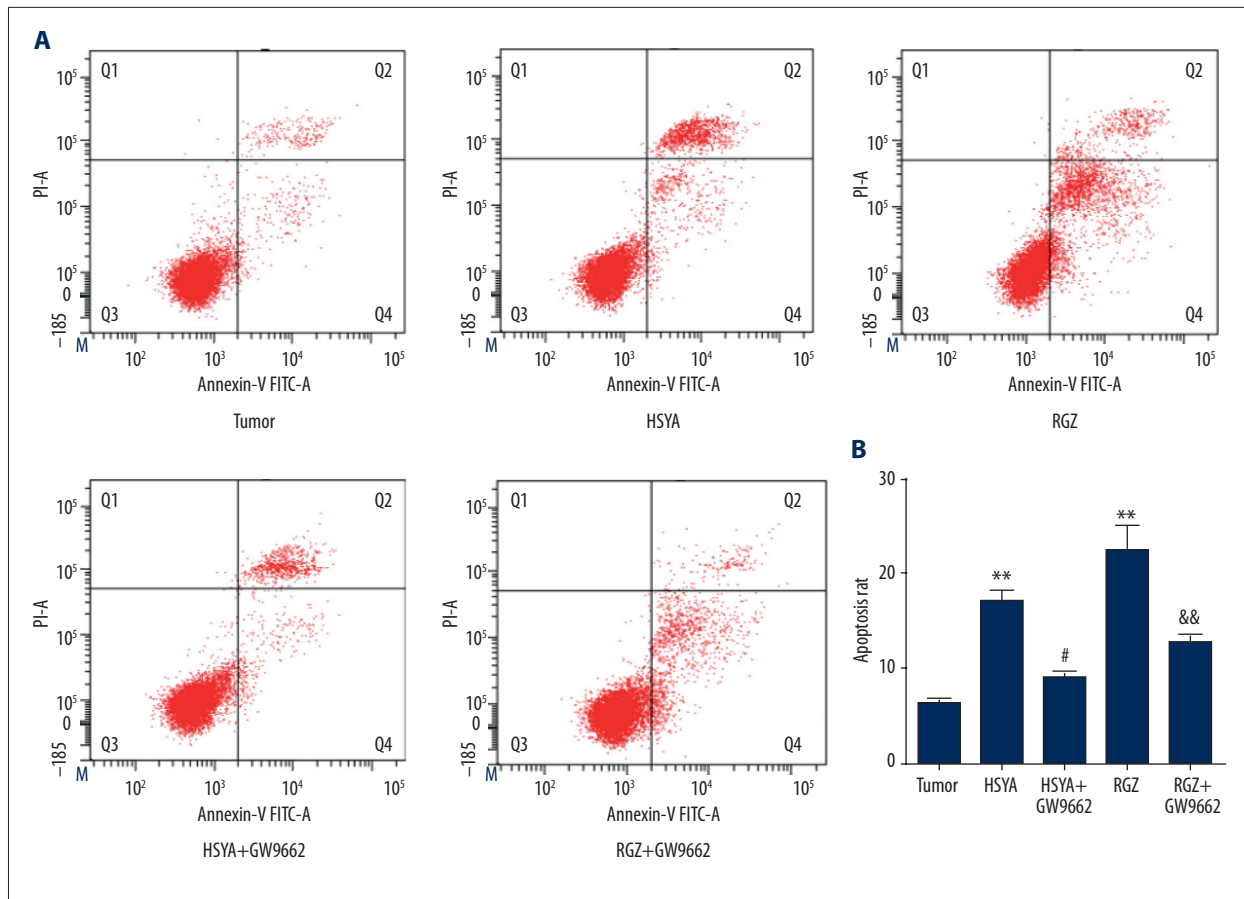


Figure 4. (A) V-FITC/PI annexin quadrant distribution of apoptosis BGC-823 cells treated with drugs at different concentrations: HSYA 100 μ M, RGZ 5 μ M, GW9662 10 μ M. (B) Compared with tumor group: ** $P<0.01$; compared with HSYA group: # $P<0.05$; compared with RGZ group: && $P<0.01$ ($n=3$).

decreased to $21.50\pm 0.55\%$ and $20.59\pm 0.20\%$ (Figure 6) for the HSYA group and RGZ group, respectively. Cells in G0/G1 phase for these 2 groups increased significantly ($P<0.01$) compared with the tumor group. For HSYA+GW9662 and RGZ+GW9662 groups, the proportions of cells in G0/G1 phase were decreased, while the proportions of cells in S phase were greatly increased ($P<0.01$) in comparison with the HSYA and RGZ groups, respectively. We found no significant differences among the 5 groups in the proportion of cells in G2/M phase. These results show that the effect of blocking cell cycle of HSYA on BGC-823 cells is dependent on activated PPAR γ .

Nuclear translocation of PPAR γ of BGC-823 cells is promoted by HSYA

PPAR γ is mainly distributed in the cytoplasm and activated upon entering the cell nucleus. Immunofluorescence staining was used to detect the distribution of PPAR γ in the cells. The nuclei were stained with DAPI (blue), while PPAR γ was stained with antibody-labeled with FITC (green). The results show that the nuclei of all groups were stained blue (Figure 7). PPAR γ

was highly distributed in the cytoplasm in the tumor group because green fluorescence was mainly observed in the cytoplasmic domain. After treatment with HSYA and RGZ, PPAR γ was activated and enriched in the nucleus instead of cytoplasm. However, PPAR γ was redistributed in the cytoplasm again with treatment of GW9662, which inactivates PPAR γ . These results show that HSYA promotes nuclear translocation of PPAR γ of BGC-823 cells.

Expression levels of PPAR γ and caspase-3 in BGC-823 cells are increased by HSYA

Caspase family members play a critical role in apoptotic pathways. Activation of caspase-3 is thought to cause a series of downstream caspases cascade reactions, ultimately leading to cell apoptosis. RT-qPCR assay was used to measure the expression of the intracellular critical apoptotic factors caspase-3 and PPAR γ to determine the effects of HSYA treatment on BGC-823 cells. As shown in Figures 8 and 9, the mRNA expression levels of caspase-3 and PPAR γ in the HSYA group and RGZ groups were significantly increased ($P<0.01$) compared with the tumor

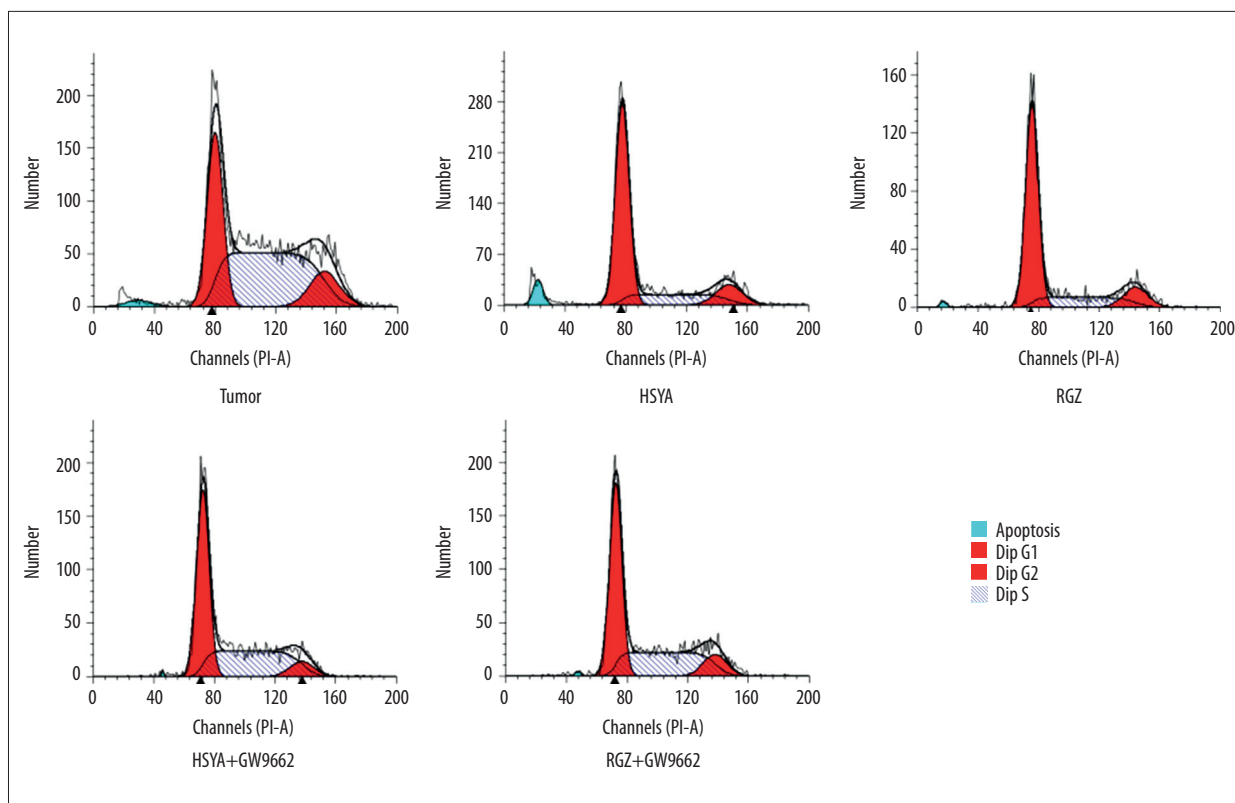


Figure 5. Distributions of cell cycle BGC-823 cells treated with drugs at different concentrations: HSYA 100 μ M, RGZ 5 μ M, GW9662 10 μ M (n=3).

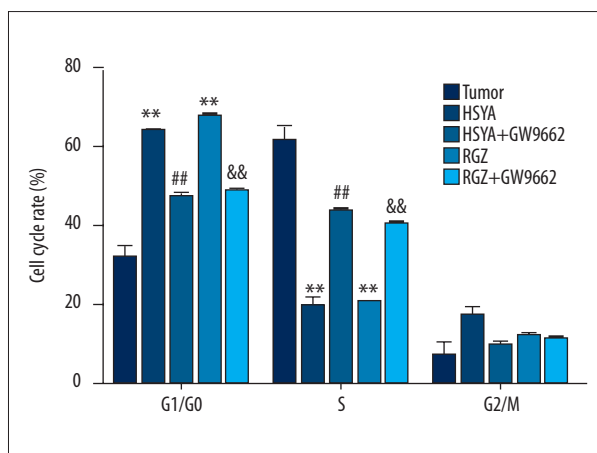


Figure 6. Effect of HSYA on BGC-823 cells cycle BGC-823 cells treated with drugs at different concentrations: HSYA 100 μ M, RGZ 5 μ M, GW9662 10 μ M. Compared with tumor group: ** P<0.01; compared with HSYA group: ## P<0.01; compared with RGZ group: && P<0.01 (n=3).

group, but mRNA expression levels were decreased (P<0.01) with GW9662 treatments to a similar extent as in the tumor group. These results show that HSYA increases expression levels of PPAR γ and caspase-3 in BGC-823 cells.

Discussion

In most cases, gastric cancers are diagnosed at the advanced stage. The overall complication occurrence rate of gastric cancer reaches 41%. The 5-year overall survival (OS) and recurrence-free survival (RFS) rates of patients with complications were 27% and 23%, much lower than the 43% and 40% in patients without complications [21]. Apoptosis is a popular research focus in the pathogenesis of cancer. Shimada et al. [22] found that PPAR γ agonist RGZ can induce apoptosis of colon cancer cells, and activated PPAR γ can increase the activity of caspase-3 in human malignant astrocytoma cells [23]. However, the relationship between PPAR γ and apoptosis of tumor cells is unclear.

Studies have reported that natural anti-cancer agents have powerful effects in controlling cancers [24–26]. Our group has focussed on anti-tumor research of HSYA for almost a decade, and we found that HSYA suppresses tumor growth by inhibiting cell proliferation [12,13] and angiogenesis [4,13,14,27], and inducing cell apoptosis. In the present study, MTT assay showed that HSYA and PPAR- γ agonist RGZ significantly inhibited BGC-823 cell proliferation. Certain concentrations of HSYA and RGZ directly induced BGC-823 cell cycle arrest at G0/G1 phase, instead of entering S phase to synthesize DNA.

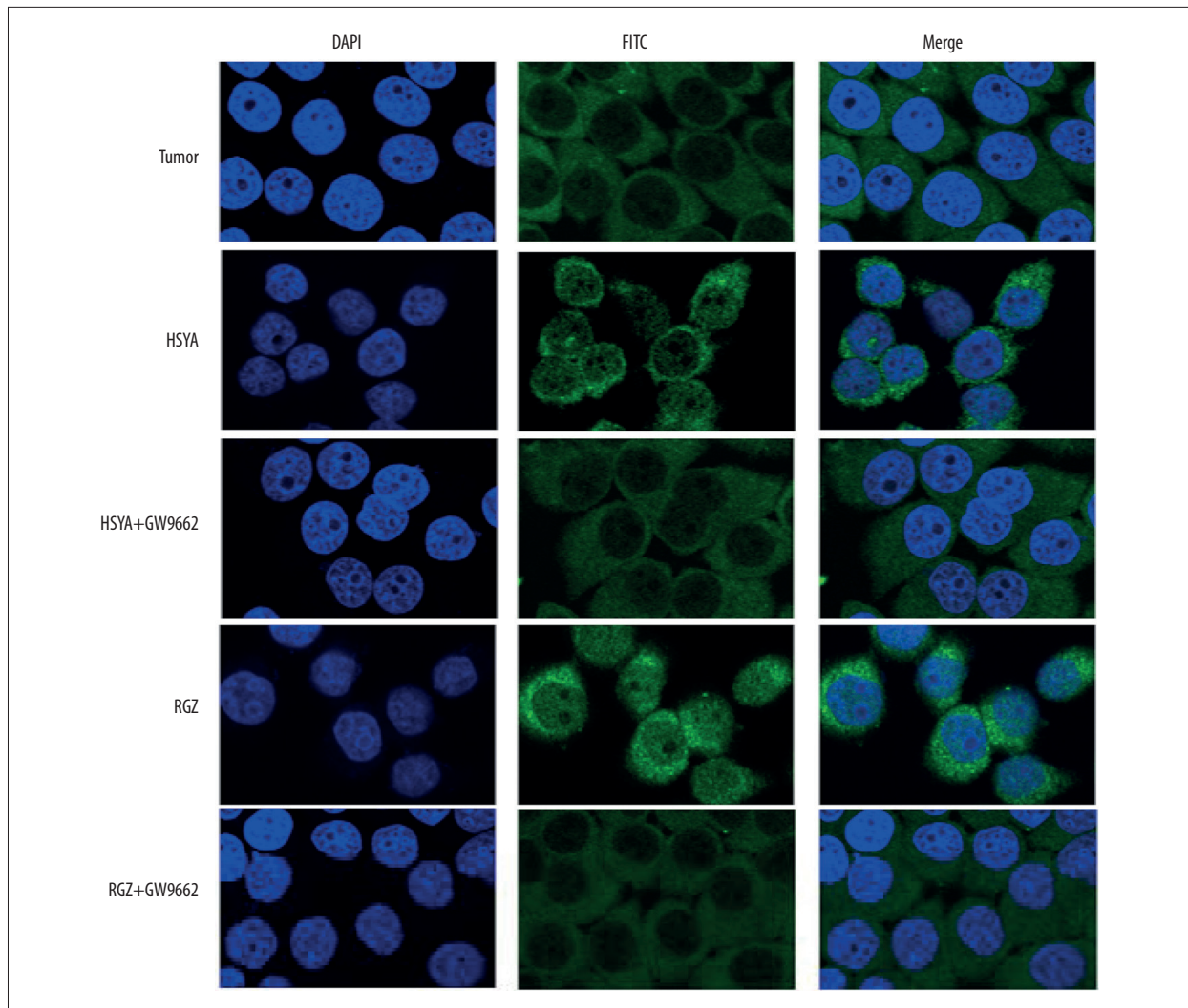


Figure 7. Distributions of PPAR γ subcellular localization ($\times 600$) BGC-823 cells treated with drugs at different concentrations: HSYA 100 μ M, RGZ 5 μ M, GW9662 10 μ M. The nuclei were stained with DAPI (blue), while the PPAR γ was stained with antibody labeled with FITC (green) (n=3).

Moreover, PPAR- γ inhibitor GW9662 disrupted the effects of HSYA and RGZ on cells. Therefore, we assume that PPAR- γ activation might be related to the inhibitory effect of HSYA on proliferation and cell cycle of tumor cells.

Peroxisome proliferator-activated receptors (PPARs) are transcription factors belonging to the nuclear hormone receptor family, which are mainly distributed in the cytoplasm. However, PPARs can be activated to enter the cell nucleus upon ligand binding. According to previous studies, PPARs are able to affect many biological functions, including inflammation, cell survival, and differentiation [28–30]. PPAR γ is an important member of the PPARs family, which is expressed in a variety of primary tumors, including gastric cancer, colon cancer, and pancreatic cancer [31–33]. PPAR γ has an anti-tumor effect on solid tumors via inhibiting tumor cell proliferation, inducing tumor cell

apoptosis, and inhibiting angiogenesis [34–36]. Wei et al. [19] reported that isoflavone and daidzein have a similar promoting effect on nuclear transfer compared with RGZ in the process of human prostate cancer DU-145 cell apoptosis. In our study, we revealed that expression level of PPAR γ was increased by treatment with HSYA and RGZ, and the nuclear transfer of PPAR γ was also promoted. To be more precise, PPAR γ is mainly expressed in the nucleus. Furthermore, PPAR γ inhibitor GW9662 was found to disrupt the effects of HSYA and RGZ, suggesting that HSYA may activate PPAR γ in BGC-823 cells.

The mechanism of apoptosis by HSYA may be related to activation of the mitochondrial apoptotic pathway and regulation of expressions of Bcl-2, Bax, and p53 [12]. Caspase family members play a critical role in the apoptotic pathway, and are mainly involved in a series of caspase activations, which

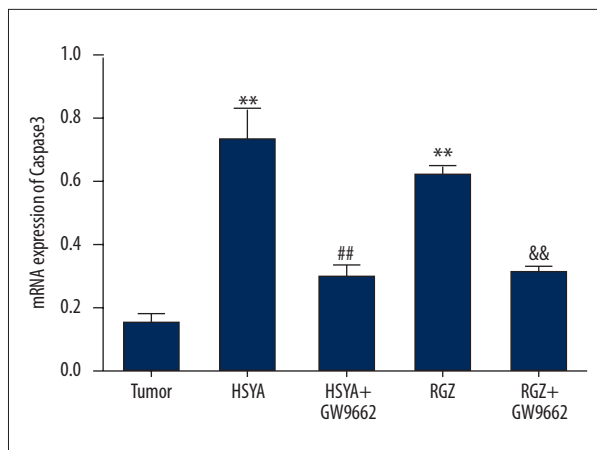


Figure 8. Effect of HSYA on caspase-3 mRNA expression in BGC-823 cells treated with drugs at different concentrations: HSYA 100 μ M, RGZ 5 μ M, GW9662 10 μ M. Compared with tumor group: ** $P < 0.01$; compared with HSYA group: ## $P < 0.01$; compared with RGZ group: && $P < 0.01$ (n=3).

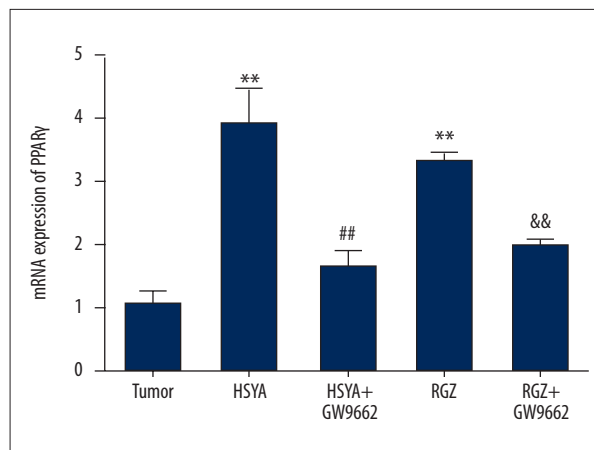


Figure 9. Effect of HSYA on PPAR γ mRNA expression in BGC-823 cells treated with drugs at different concentrations: HSYA 100 μ M, RGZ 5 μ M, GW9662 10 μ M. Compared with tumor group: ** $P < 0.01$; compared with HSYA group: ## $P < 0.01$; compared with RGZ group: && $P < 0.01$ (n=3).

are regulated to the extrinsic pathway and the intrinsic pathway. The caspase-8 of the extrinsic pathway and caspase-9 of the intrinsic pathway were activated and gathered together in caspase-3, and activated caspase-3 caused a series of downstream caspases cascade reactions, then ultimately induced apoptosis through the inhibition of DNA repair, nuclear fragmentation, cell shrinkage, and cell membrane bubble [37,38]. Yuan et al. [39] demonstrated that the expression of PPAR γ and caspase-3 was significantly increased by CLA in human breast cancer SKBr3 cells, elucidating the synergistic relationship between them via treatment with GW9662 (PPAR γ inhibitor). In the present study, we revealed that apoptotic rates of HSYA and RGZ groups were significantly increased compared with the tumor group. We further demonstrated that the expression of caspase-3 mRNA can be significantly promoted by HSYA and RGZ in tumor cells. The effects of HSYA and RGZ were diminished by PPAR γ inhibitor GW9662, suggesting that

HSYA activates PPAR γ , inducing caspase-3 expression, and subsequently promoting BGC-823 cell apoptosis.

Conclusions

We showed the inhibitory effect of HSYA on the proliferation of BGC-823 cells, which results in activating PPAR γ -dependent cell cycle block and cell apoptosis. Our results suggest that PPAR γ is a specific type of HSYA that induces apoptosis of BGC-823 cells, providing a theoretical insight into the development of HSYA as a potential PPAR γ agonist and a clinical cancer treatment.

Conflicts of interests

None.

References:

- Hanahan D, Weinberg RA: Hallmarks of cancer: The next generation. *Cell*, 2011; 144: 646–74
- Jin GL, Zhang Q: The anti-cancer traditional Chinese Medicine. 1st ed. Shanghai (China): Shanghai Scientific & Technical Publishers, 2011; 138
- Zhang JC, Chen KJ: The academic thought and medical record. Beijing (China): Peking University Medical Press, 2007; 237–38
- Li J: Hydroxysafflor yellow A suppresses inflammatory responses of BV2 microglia after oxygen-glucose deprivation. *Neurosci Lett*, 2013; 535(1): 51
- Yang F, Li J, Zhu J et al: Hydroxysafflor yellow A inhibits angiogenesis of hepato-ocellular carcinoma via blocking ERK/MAPK and NF- κ B signaling pathway in H-22 tumor-bearing mice. *Eur J Pharmacol*, 2015; 754: 105–14
- Chen TT, Du YJ, Liu XL et al: [Inhibitory action of hydroxysafflor yellow A on inflammatory signal transduction pathway related factors in rats with cerebral cortex ischemia.] *Yao Xue Xue Bao*. 2008; 43(6): 570–75 [in Chinese]
- Liu YG, Li FJ, Tang F: [Protective effects of hydroxy safflor yellow A on myocardial ischemia reperfusion injury in rats.] *Pharmacology and Clinics of Chinese Materia Medica*, 2015; (1): 71–74 [in Chinese]
- Zhang Q, Niu X, Yan Y et al: Research on the mechanism of hydroxysafflor yellow A in inhibiting angiogenesis. *J Beijing Univ Trad Chinese Med*, 2004; 27: 25–29
- Wang J, Zhang Q, Gu LG et al: Effect of hydroxy safflor yellow A on the cell cycle and apoptosis of human umbilical vein endothelial cells with the stimulus of tumor cell conditioned medium. *J Beijing Univ Trad Chinese Med*, 2008; 31: 741–44
- Wang J, Wang JJ, Wang XX et al: Molecular mechanism of inhibition of the abnormal proliferation of human umbilical vein endothelial cells by hydroxysafflor-yellow A. *Pharmaceutical Biology*, 2016; 1–8

11. Wang J, Zhang Q, Xie H et al: Effect of hydroxy safflor Yellow A on the proliferation of human umbilical vein endothelial cells with the stimulus of tumor cell conditioned medium. *China Journal of Traditional Chinese Medicine and Pharmacy*, 2009; 24: 572–75
12. Si N, Wang JJ, Xu YY et al: Inductive effects of hydroxyl safflower yellow A on apoptosis in abnormal human umbilical vein endothelial cells via the mitochondrial pathway. *Journal of Traditional Chinese Medical Sciences*, 2015; 2: 25–31
13. Wang JJ, Hu JH, Yu X et al: Effects of hydroxy safflor yellow A on the cell proliferation, apoptosis and cycle of cultured human gastric cancer cell. *China Journal of Traditional Chinese Medicine and Pharmacy*, 2016; (9): 3738–41
14. Xi SY, Zhang Q, Xie H et al: Effects of hydroxy safflower yellow A on the expression of VEGF and bFGF mRNA on transplantation tumor of human gastric adenocarcinoma BGC-823 in nude mice. *China Journal of Chinese Materia*, 2009; 34(5): 605–9
15. Xi SY, Zhang Q, Liu ZY et al: Inhibitory effect of hydroxy safflower yellow A on transplantation tumor of human gastric adenocarcinoma cell BGC-823 in nude mice. *J Beijing Univ Trad Chinese Med*, 2009;32(5): 331–35
16. Yuan XL, He F, Chen Q et al: Effects of conjugated linoleic acid monomer on apoptosis of breast cancer cell line SKBr3 induced by PPAR signal pathway. *Progress in Biochemistry and Biophysics*, 2009; 36(4): 491–99
17. Zander T, Kraus JA, Grommes C et al: Induction of apoptosis in human and rat glioma by agonists of the nuclear receptor PPAR gamma. *J Neurochem*, 2002; 81(5): 1052–60
18. Chen JW, Ren YZ: Effect of PPAR γ on PTEN expression in human pancreatic cancer cells. *Chinese Journal of Cellular and Molecular Immunology*, 2010; 24(8): 828–29
19. Wei HM, Zhou J, Rong R, Zhu JD: Soy isoflavones promotes apoptosis in human prostate cancer DU-145 cells through PPAR γ activation. *J Third Mil Med Univ*, 2012; (01): 29–33
20. Zhang M, Peng L, Miao ZJ et al: Effect of rosiglitazone on VEGF protein expression in SMMC-7721 cells. *Acta Cancer Res*, 2010; 37(3): 298–301
21. Jin LX, Sanford DE, Ili M H S et al: Interaction of postoperative morbidity and receipt of adjuvant therapy on long-term survival after resection for gastric adenocarcinoma. *Ann Surg Oncol*, 2011; 23(8): 1–11
22. Shimada T, Kojima K, Yoshiura K et al: Characteristics of the peroxisome proliferator activated receptor gamma (PPARgamma) ligand induced apoptosis in colon cancer cells. *Gut*, 2002; 50(5): 664–58
23. Chattopadhyay N, Singh D P, Heese O et al: Expression of peroxisome proliferator-activated receptors (PPARs) in human astrocytic cells: PPARgamma agonists as inducers of apoptosis. *J Neurosci Res*, 2000; 61(1): 67–74
24. Zhu X, Jiang H, Li J et al: Anticancer effects of *Paris saponins* by apoptosis and PI3K/AKT pathway in gefitinib-resistant non-small cell lung cancer. *Med Sci Monit*, 2016; 22: 1435–41
25. Song S, Du L, Jiang H et al: Paris saponin I sensitizes gastric cancer cell lines to cisplatin via cell cycle arrest and apoptosis. *Med Sci Monit*, 2016; 22: 3798–803
26. Zheng R, Rao Y, Jiang H et al: Therapeutic potential of Ginsenoside Rg3 via inhibiting Notch/HES1 pathway in lung cancer cells. *Transl Cancer Res*, 2016; 5(4): 464–69
27. Wang XX, Wang JJ, Wang X et al: Hydroxysafflor yellow A inhibited abnormal proliferation of vascular endothelial cells. *J Beijing Univ Trad Chinese Med*, 2016; 39(8): 679–84
28. Alqahtani S, Mahmoud A M: Gamma-glutamylcysteine ethyl ester protects against cyclophosphamide – induced liver injury and hematologic alterations via upregulation of PPAR γ and attenuation of oxidative stress, inflammation, and apoptosis. *Oxid Med Cell Longev*, 2016; 2016: 4016209
29. Liu H, Rose M E, Culver S et al: Rosiglitazone attenuates inflammation and C-A3 neuronal loss following traumatic brain injury in rats. *Biochem Biophys Res Commun*, 2016; 472(4): 648–55
30. Lutzen U, Zhao Y, Lucht K et al: Activation of the cell membrane angiotensin AT2 receptors in human leiomyosarcoma cells induces differentiation and apoptosis by a PPAR γ – dependent mechanism. *Neoplasma*, 2017; 64(3): 395–405
31. Sato H, Ishihara S, Kawashima K et al: Expression of peroxisome proliferator-activated receptor (PPAR) gamma in gastric cancer and inhibitory effects of PPAR gamma agonists. *Br J Cancer*, 2000; 83(10): 1394–400
32. Yang W-L, Frucht H: Activation of the PPAR pathway induces apoptosis and C-OX-2 inhibition in HT-29 human colon cancer cells. *Carcinogenesis*, 2001; 22(9): 1379–83
33. Motomura W, Okumura T, Takahashi N, Obara T, Kohgo Y: Activation of peroxisome proliferator-activated receptor by troglitazone inhibits cell growth through the increase of p27Kip1 in human pancreatic carcinoma cells. *Cancer Res*, 2000; 60(19): 5558–64
34. Yang LJ, Yuan JL, Liu LW et al: Alpha-linolenic acid inhibits human renal cell carcinoma cell; proliferation through PPAR-gamma activation and COX-2 inhibition. *Oncol Lett*, 2013; 6(1): 197–202
35. Ramer R, Heinemann K, Merkord J et al: COX-2 and PPAR-gamma confer cannabidiol-induced apoptosis of human lung cancer cells. *Mol Cancer Ther*, 2013; 12(1): 69–82
36. Qin L, Ren Y, Chen A M et al: Peroxisome proliferator-activated receptor gamma ligands inhibit VEGF-mediated vasculogenic mimicry of prostate cancer through the AKT signaling pathway. *Mol Med Rep*, 2014; 10(1): 276–82
37. Hengartner MO: Apoptosis: Corraling the corpses. *Cell*, 2001; 104(3): 325–28
38. Danial NN, Korsmeyer SJ: Cell death: Critical tumor points. *Cell*, 2004; 116(2): 205–19
39. Ghobrial IM, Witzig TE, Adjei AA: Targeting apoptosis pathways in cancer therapy. *Cancer J Clin*, 2005; 55(3): 178–94